Synthesis and Characterization of Two Novel Large-Pore Crystalline Vanadosilicates

Paula Brandão,[†] Andreas Philippou,[‡] Noreen Hanif,[‡] Paulo Ribeiro-Claro,[†] Artur Ferreira,[§] Michael W. Anderson,[‡] and João Rocha*[,†]

Department of Chemistry and ESTGA, University of Aveiro, 3810-193 Aveiro, Portugal, and Department of Chemistry, UMIST, P.O. Box 88, Manchester M60 1QD, U.K.

Received July 17, 2001. Revised Manuscript Received December 5, 2001

Two novel large-pore sodium vanadosilicates (Aveiro-Manchester, structure numbers 13 and 14) containing stoichiometric amounts of vanadium (Si/V = 10 and 4, respectively) have been synthesized. Only one other example of a large-pore vanadosilicate (AM-6) is known. AM-13 and AM-14 were characterized by bulk chemical analysis (ICP); powder X-ray diffraction (XRD); scanning electron microscopy (SEM); thermogravimetric analysis (TGA); differential scanning calorimetry (DSC); N_2, *n*-hexane, benzene, and tripropylamine adsorption measurements; and Raman and diffuse reflectance ultraviolet−visible (DR UV−vis) spectroscopies. The acid−base and redox properties of these materials were assessed by 2-propanol conversion and ethanol oxidation, respectively. Both materials exhibit high selectivities to acetaldehyde, indicating that these two novel vanadosilicates are promising redox catalysts. However, because the thermal stability of AM-14 is modest (ca. 350 °C), its potential use as a catalyst is limited.

Introduction

The synthesis and characterization of microporous silicate materials with metals in various coordinations has stimulated a large amount of research in recent years.[1] The most-studied materials include microporous titanosilicates containing Ti(IV) in octahedral coordination (ETS-type materials).[2−4] ETS-10, the most prominent member of this family, contains corner-sharing TiO_6 octahedra and SiO_4 tetrahedra. Its pore structure consists of 12-rings, 7-rings, 5-rings, and 3-rings, and the material exhibits a three-dimensional wide-pore system whose minimum diameter is defined by 12-ring apertures.[2] Vanadium has been introduced in the framework of certain zeolites in small amounts. Cavansite and pentagonite, dimorphs of the mineral $Ca(VO)(Si_4O_{10})\cdot 4H_2O$ (Malheur County, Oregon), are the only known natural small-pore framework solids containing stoichiometric amounts of vanadium.[5,6] The first example of a synthetic large-pore framework vanadosilicate (AM-6), containing stoichiometric amounts of hexacoordinated vanadium was reported in 1997.[7] AM-6 is a structural analogue of ETS-10, in which titanium has been fully replaced by vanadium. Here, we report the synthesis and structural characterization of two novel large-pore sodium vanadosilicates, which we have designated AM-13 and AM-14.

Experimental Section

Synthesis. The synthesis of AM-13 and AM-14 was carried out in Teflon-lined autoclaves under static hydrothermal conditions.

Synthesis of AM-13. An alkaline solution was made by mixing 5.00 g of sodium silicate solution (8 wt % Na_2O, 27 wt % SiO_2, Merck), 9.40 g of H_2O, and 0.60 g of $Ca(OH)_2$ (Aldrich). A second solution was made by mixing 6.13 g of H_2O with 1.00 g of $VOSO_4\cdot 5H_2O$ (Merck). These two solutions were combined and stirred thoroughly.

Synthesis of AM-14. An alkaline solution was made by mixing 5.02 g of sodium silicate solution (Merck), 9.05 g of H_2O, 0.54 g of NaOH (Merck), and 0.76 g of NaCl (Aldrich). A second solution was made by mixing 6.66 g of H_2O with 1.44 g of $VOSO_4\cdot 5H_2O$ (Merck).

The AM-13 gel with a composition of 3.3 Na_2O:4.1 CaO:11.4 SiO_2:V_2O_5:419 H_2O and the AM-14 gel with a composition of 4.7 Na_2O:8.0 SiO_2:V_2O_5:276 H_2O were autoclaved for 3 days at 230 °C. The crystalline powders were filtered off, washed, and dried at room temperature.

Catalytic Tests. The experiments were performed in a fixed-bed stainless steel reactor at atmospheric pressure. The reactor length and internal diameter were 16 and 0.5 cm, respectively, and the reactor bed measured 1 cm long and had an internal diameter of 0.5 cm. The catalyst (50 mg) was activated at 350 °C for 2-propanol in a flow of argon (10 mL/min) prior to reaction. For ethanol oxidation, the catalyst (50 mg) was activated at 350 °C in a flow of air (2 mL/min) prior to reaction. The reactant was fed by a syringe pump, and the

* Address correspondence to Prof. J. Rocha, Department of Chemistry, University of Aveiro, 3810-193 Aveiro, Portugal. Fax: +351 34 370084. Tel.: +351 370730. E-mail: ROCHA@DQ.UA.PT.

[†] Department of Chemistry, University of Aveiro.

[‡] UMIST.

[§] ESTGA, University of Aveiro.

(1) Rocha, J.; Anderson, M. W. *Eur. J. Inorg. Chem*. **2000**, 801.

(2) Anderson, M. W.; Terasaki, O.; Ohsuna, T.; Philippou, A.; Mackay, S. P.; Ferreira, A.; Rocha, J.; Lidin, S. *Nature* **1994**, *367*, 347.

(3) Lin, Z.; Rocha, J.; Brandão, P.; Ferreira, A.; Esculcas, A. P.; Pedrosa de Jesus, J. D.; Anderson, M. W. *J. Phys. Chem. B* **1997**, *101*, 7114.

(4) Dadachov, M. S.; Rocha, J.; Ferreira, A.; Lin, Z.; Anderson, M. W. *Chem. Commun.* **1997**, 2371.

(5) Evans, H. T., Jr. *Am. Mineral. B.* **1973**, *58*, 412.

(6) Rinaldi, R.; Pluth, J. J.; Smith, J. V. *Acta Crystallogr. B* **1975**, *31*, 1598.

(7) Rocha, J.; Brandão, P.; Lin, Z.; Anderson, M. W.; Alfredsson, V.; Terasaki, O. *Angew. Chem., Int. Ed. Engl.* **1997**, *36*, 100.

10.1021/cm010613q CCC: $22.00
Published on Web 02/09/2002

Table 1. Powder XRD Data of AM-13

d (Å)	I/I_0	*d* (Å)	I/I_0
13.663	32	3.901	1
13.347	39	3.717	21
13.102	42	3.581	4
8.442	2	3.546	10
7.086	73	3.421	17
6.536	40	3.367	66
6.247	3	3.271	25
5.875	6	3.118	78
5.330	24	3.039	16
4.809	63	2.969	93
4.365	6	2.955	100
4.159	2		

products were analyzed by means of gas chromatography with a 30-m-long capillary column (DP1 fused-silica phase) and a FID (flame ionization detector).

Characterization. Powder XRD data were collected on a X′Pert MPD Philips diffractometer (Cu K_α X-radiation) with a curved graphite monochromator, an automatic divergence slit (irradiated length = 20.00 mm), a progressive receiving slit (slit height = 0.05 mm), and a flat plate sample holder in a Bragg−Brentano para-focusing optics configuration. Intensity data were collected by the step-counting method (step = 0.02°, time = 38 s) in the range $2\theta = 3-32°$. X-ray diffraction pattern auto-indexing was performed with the CRYSFIRE system[8] from the first 20 resolved lines and checked with the Chekcell package.[9]

SEM images were recorded on a Hitachi S-4100 field emission gun tungsten filament working with a voltage of 25 000 V. The in situ work was carried out using an Anton Parr high-temperature chamber and a 10 °C/min heating rate. Bulk chemical analysis was performed by inductively coupled plasma atomic emission spectroscopy (ICP-AES). TGA and DSC curves were measured with TGA-50 and DSC Shimadzu analyzers. The samples were heated under air at a rate of 2 °C/min. Surface area and pore volume measurements were performed on a Micromeritics ASAP 2010 V1.01 B automatic instrument by adsorption of nitrogen gas at 77 K. Before the measurements, the samples were outgassed overnight at 573 K. Pore size distributions were determined using the density functional theory (DFT) Plus Software for data files generated from the ASAP instrument. Adsorption isotherms of *n*-hexane, benzene, and tripropylamine were measured at room temperature using a gravimetric adsorption apparatus equipped with a CI electronic MK2-M5 microbalance and an Edwards Barocel pressure sensor. Before analysis, the solids (typically around 0.02 g) were outgassed at 573 K overnight to a residual pressure of ca. 10^{-4} mbar. DR UV−vis spectra were recorded on a Jasco V-560 PC spectrometer using $BaSO_4$ as the reference material. The Raman spectra were recorded on a triple monochromator (Jobin Yvon T 64000) using a CCD (Jobin Yvon Spectraview 2D) detector. The samples were sealed in Kimax glass capillaries (i.d. = 0.8 mm). The samples were illuminated by the 514.5-nm line of an Ar^+ laser (Coherent-Inova 90) with a power of 50 mW at the sample position. The entry slit of the spectrometer was set to 200 μm, giving a resolution of approximately 3 cm^{-1}. The error in wavenumbers is estimated to be smaller than 1 cm^{-1}.

Results and Discussion

Powder XRD. The powder XRD patterns of AM-13 and AM-14 (Tables 1 and 2, respectively, and Figure 1) indicate that the structures of these materials are, to the best of our knowledge, not found among mineral or synthetic vanadosilicates or related materials. Because of strong orientation effects and relatively broad reflection lines, it is not easy to index the powder XRD patterns of these materials, and thus, the cells given here are only tentative. The AM-13 and AM-14 cells are both triclinic with parameters of (AM-13) $a = 9.736$ Å, $b = 15.629$ Å, $c = 15.730$ Å, $\alpha = 60.67°$, $\beta = 79.19°$, $\gamma = 75.63°$ ($V = 2015$ Å^3) and (AM-14) $a = 15.818$ Å, $b = 31.018$ Å, $c = 11.754$ Å, $\alpha = 91.37°$, $\beta = 100.62°$, $\gamma = 76.99°$ ($V = 5522$ Å^3).

Table 2. Powder XRD Data of AM-14

d (Å)	I/I_0	*d* (Å)	I/I_0
14.839	87	4.989	11
12.082	36	4.871	3
11.533	39	4.734	4
10.835	10	4.566	4
9.461	14	4.493	6
9.263	27	4.330	6
8.961	3	4.280	4
7.869	10	4.016	12
7.668	25	3.849	100
7.539	15	3.720	89
6.934	7	3.617	36
6.814	3	3.590	25
6.073	4	3.558	13
6.014	3	3.536	11
5.777	7	3.420	4
5.603	11	3.355	6
5.426	29	3.181	45
5.282	18	3.134	23
5.180	3	3.050	12
5.069	3		

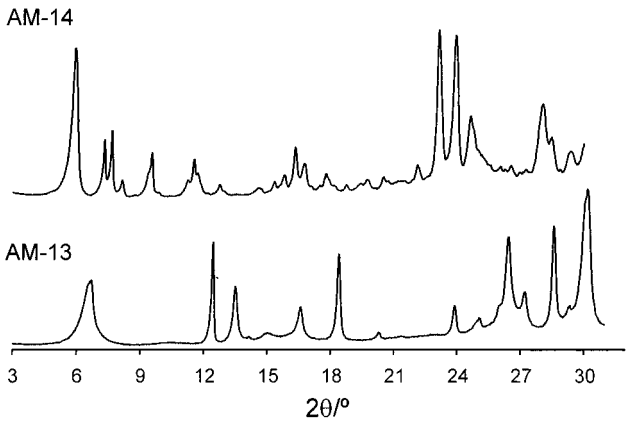

Figure 1. Powder XRD patterns of AM-13 and AM-14.

SEM, TEM, and ICP. SEM images of the AM-13 and AM-14 samples are presented in Figure 2. AM-13 consists of ca. 5-μm crystallites in the shape of needles. AM-14 crystals are thin plates with a size of ca. 1−2 μm. The TEM image of AM-14 is shown in Figure 3, where the white dots are the pores. The size of the pore estimated from this image is ca. 6.5 Å and is in accord with the pore size of 6.8 Å derived from the N_2 adsorption isotherm. AM-13 crystals are thin needles, making it difficult to obtain TEM images. Bulk chemical analysis (ICP) of AM-14 yields Si/V and Na/V molar ratios of 4 and 2, respectively. This gives the ideal formula for the dehydrated material of $Na_2Si_4VO_{11}$, where vanadium is present as V(IV). For AM-13, ICP yields Si/V, Na/Ca, and Na/V molar ratios of ca. 10, 0.5, and 0.5, respectively. Assuming all vanadium is present as V(IV), we propose for AM-13 the ideal formula $HNaCa_2Si_{20}V_2O_{47}$. When the synthesis time was in-

(8) Shirley, R. *The CRYSFIRE System for Automatic Powder Indexing: User's Manual*; The Lattice Press: Surrey, U.K., 2000.

(9) Laugier, J.; Bochu, B. *Programme D'affinement des Paramètres de Maille à Partir d'un Diagramme de Poudre*; Laboratoire des Matériaux et du Génie Physique, École Nationale Supérieure de Physique de Grenoble (INPG): Saint Martin d'Hères, France.

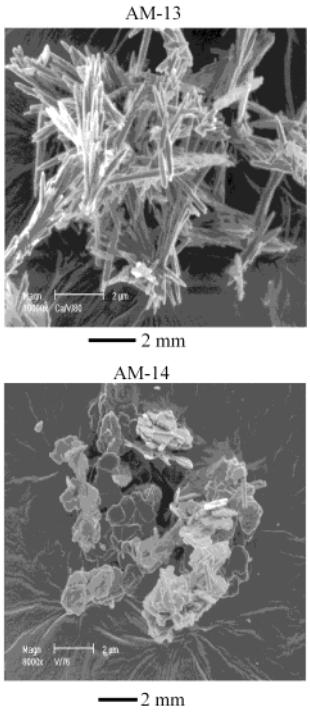

Figure 2. SEM images of AM-13 and AM-14.

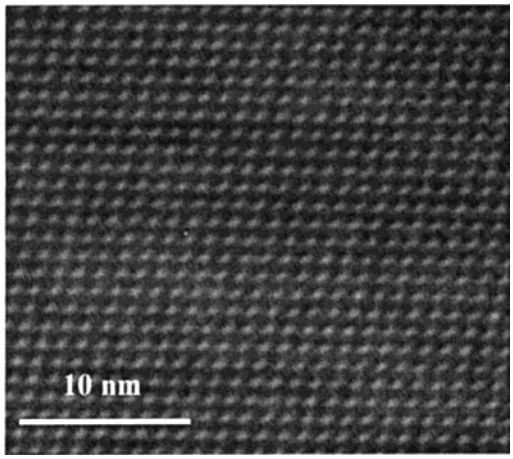

Figure 3. TEM image of AM-14.

creased from 1 day to 3 days, AM-13 samples were contaminated with the synthetic rhodesite ($HNaCa_2Si_8O_{19}{\cdot}xH_2O$).[10]

TGA and DSC. Figure 4 shows TGA and DSC curves, recorded under air, for AM-13 and AM-14. The former reveal gradual weight losses between room temperature and 350 °C. The total mass loss between 30 and 700 °C are ca. 13% (AM-13) and 15% (AM-14). The DSC curves of AM-13 and AM-14 exhibit broad endothermic peaks centered at ca. 60 °C (with a shoulder at ca. 120 °C for AM-14) ascribed to the loss of water on the external surface of the crystals and in the micropores. Whereas AM-14 exhibits a sharp exothermic peak at 358 °C, probably associated with the collapse of the structure, AM-13 displays only a faint and broad exothermic peak in this region. The thermal stability of the materials was further investigated using variable-temperature (25−700 °C) in situ powder XRD. When calcined in a vacuum, both materials retain structural integrity up to about 600 °C (data not shown). However, upon calcination in air, AM-13 is stable up to temperatures in excess of 400 °C, whereas the AM-14 structure seems to collapse entirely after the 360 °C exothermic event (Figure 5).

(10) Rocha, J.; Ferreira, P.; Lin, Z.; Brandão, P.; Ferreira, A.; Pedrosa de Jesus, J. D. *J. Phys. Chem. B* **1998**, *102*, 4739.

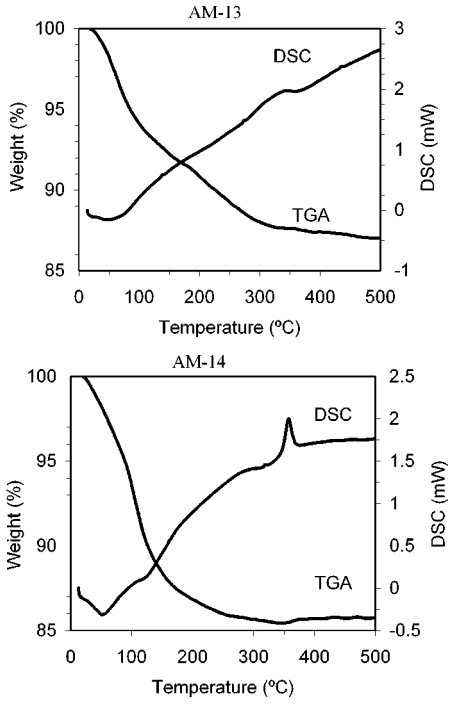

Figure 4. TGA and DSC curves, recorded in air, of AM-13 and AM-14.

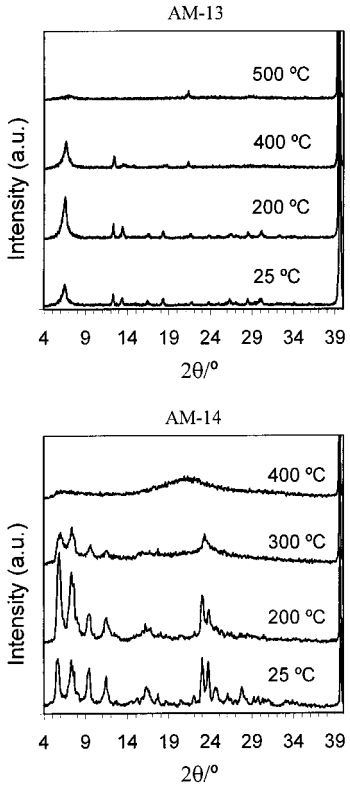

Figure 5. Powder XRD patterns of AM-13 and AM-14 recorded in situ at different temperatures.

Adsorption Measurements. Figure 6 shows the N_2 adsorption/desorption isotherms of AM-13 and AM-14.

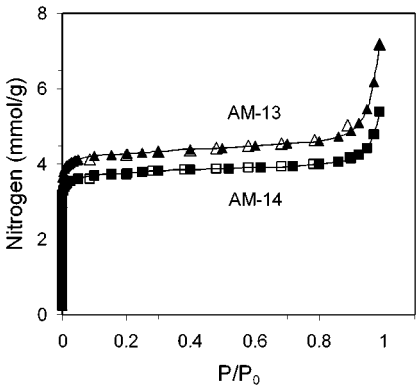

Figure 6. Nitrogen adsorption (solid symbols) and desorption (open symbols) isotherms of AM-13 and AM-14.

Table 3. Adsorption Data and Textural Properties of AM-13 and AM-14

catalyst	*n*-hexane (mmol/g)	benzene (mmol/g)	$(C_3H_7)_3N$[a] (mmol/g)	V_P (cm^3/g)	S_{Lang} (m^2/g)
AM-13	1.24	0.83	0.54	0.13	420
AM-14	1.34	1.11	0.83	0.11	377

[a] At 25 °C and P/P_0=0.6, values recorded after 3.5 h of equilibration.

For both solids, the isotherms are of type I, characteristic of microporous materials. At high relative pressures, the N_2 uptake increases, which might be due to the presence of some mesopores. AM-13 and AM-14 show similar and very narrow pore size distributions, with an average pore diameter of 6.8 Å, indicating that they are large-pore materials. The *n*-hexane (4.3 Å) and benzene (5.85 Å)[11] room-temperature adsorption isotherms are of type I, with maximum uptakes at a relative pressure (P/P_0) of 0.5 varying between 0.83 (AM-13, benzene) and 1.34 (AM-14, *n*-hexane) mmol/g (Table 3). These results are comparable to those reported for common large-pore zeolites such as X, Y, and L.[11] The largest molecule adsorbed by the AM materials is tripropylamine [$(C_3H_7)_3N$], which has a kinetic diameter of 8.1 Å (Table 3).[11] The Langmuir surface areas (S_{Lang}) and micropore volumes (V_P) estimated from *t* plots are given in Table 3.

Raman Spectroscopy. The Raman spectrum of microporous framework vanadosilicate AM-6 (Figure 7) contains a strong and sharp band at ca. 870 cm^{-1}, ascribed to relatively undistorted VO_6 octahedra.[7] AM-14 displays a similar sharp band at 890 cm^{-1}. This indicates that the vanadium environments in AM-6 and AM-14 are similar. The Raman spectrum of AM-13 does not exhibit the sharp band at 870−890 cm^{-1}, which might indicate a different local vanadium environment. Raman bands associated with V=O bonds usually appear at 900−1000 cm^{-1}.[12] The AM-13 Raman spectrum has a broad weak band at 998 cm^{-1}, which could be ascribed to V=O bonds. No crystalline V_2O_5 phase is detected as no Raman bands are present at 994, 701, 526, and 284 cm^{-1}.

Diffuse-Reflectance UV−Visible Spectroscopy. DR UV−vis spectroscopy has been used extensively to acquire information on the different vanadium species present in molecular sieves.[13−22] AM-6 contains hexacoordinated V(IV) and hence is a suitable DR UV-vis reference compound. The DR UV−vis spectrum of AM-6 (Figure 8) shows broad bands centered at ca. 600, 420−430, and 270 nm. The absorption bands at 600 and 420−430 nm are assigned to the d−d transitions of V(IV), and thus, the sample is green-colored. The charge transfer (CT) associated with O-to-V(IV) electron transfer occurs in the range 220−270 nm. AM-6, AM-13, and AM-14 display similar DR UV−vis absorption bands. Together, these results suggest that AM-13 and AM-14 contain V(IV). Although the spectra of the two materials are similar, there are some differences. For AM-14, the absorption bands at 420−430 and 270 nm, present in AM-6, are shifted to 445 (d−d transitions) and 230 nm (CT), respectively. AM-13 has absorption bands at 445 nm and in the UV at 210 and 234 nm. Both AM-13 and AM-14 have a band at 320 nm that is not observed for AM-6. This band, which is stronger for the former material, might be due to V(V) ions in tetrahedral coordination. Indeed, materials with tetracoordinated V(V), such as NH_4VO_3, show absorption bands at ca.

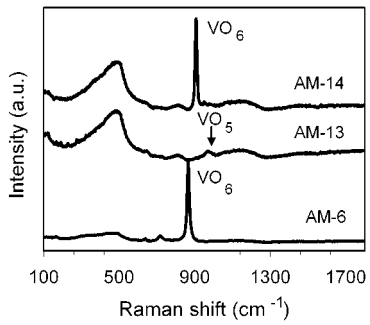

Figure 7. Raman spectra of AM-6, AM-13, and AM-14 measured at room temperature.

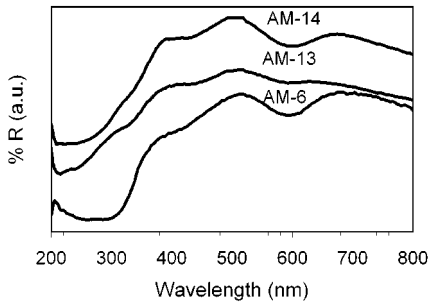

Figure 8. Diffuse reflectance UV−vis spectra of AM-6, AM-13, and AM-14.

(11) Breck, D. W. *Zeolite and Molecular Sieves*; John Wiley & Sons: New York, 1974; Chapter 8.
(12) Hardcastle, F. D.; Wachs, I. E. *J. Phys. Chem.* **1991**, *95*, 5031.
(13) Dutoit, D. C. M.; Schneider, M.; Fabrizioli, P.; Baiker, A. *Chem. Mater.* **1996**, *8*, 734.
(14) Sen, T.; Ramaswamy, V.; Ganapathy, S.; Rajamohanan, P. R.; Sivasanker, S. *J. Phys. Chem.* **1996**, *100*, 3809.
(15) Luan, Z.; Xu, J.; He, H.; Klinowski, J.; Kevan, L. *J. Phys. Chem.* **1996**, *100*, 19595.
(16) Luan, Z.; Zhao, D.; Kevan; L. *Microporous Mesoporous Mater.* **1998**, *20*, 93.
(17) Catana, G.; Rao, R. R.; Weckhuysen, B. M.; Van Der Voort, P.; Vansant, E.; Schoonheydt, R. A. *J. Phys. Chem. B* **1998**, *102*, 8005.
(18) Wei, D.; Wang, H.; Feng, X.; Chuch, W.; Ravikovitch, P.; Lyubovsky, M.; Li, C.; Takeguchi, T.; Haller, G. L. *J. Phys. Chem. B* **1999**, *103*, 2113.
(19) Dzwigaj, S.; Massiani, P.; Davidson, A.; Che, M. *J. Mol. Catal. A: Chem.* **2000**, *155*, 169.
(20) Zahedi-Niaki, M. H.; Zaidi, S. M. J.; Kaliaguine, S. *Appl. Catal. A: Gen.* **2000**, *196*, 9.
(21) Luan, Z.; Bae, J. Y.; Kevan; L. *Chem. Mater.* **2000**, *12*, 3202.
(22) Dai, L. X.; Tabata, K.; Suzuki, E.; Tatsumi, T. *Chem. Mater.* **2001**, *13*, 208.

Table 4. Conversion and Product Selectivities (wt %) of Isopropanol[a] and Ethanol Oxidation[b] over AM-13 and AM-14

	AM-13	AM-14	AM-13	AM-14
	2-propanol conversion		ethanol conversion	
	70.3	26.0	37.4	34.1
	selectivity			
acetone	10.0	84.2	−	−
propene	90.0	15.8	−	−
acetaldehyde	−	−	57.4	85.0
ethyl acetate	−	−	2.7	9.9
ethene	−	−	31.6	2.7
diethyl ether	−	−	6.9	1.1

[a] Catalyst activation at $T = 350$ °C and $P = 1$ atm for 3 h. $T_{reaction} = 350$ °C, TOS = 60 min, WHSV = 2 h^{-1}, carrier gas = argon. [b] Catalyst activation at $T = 350$ °C and $P = 1$ atm for 3 h. $T_{reaction} = 300$ °C, TOS = 60 min, WHSV = 0.4 h^{-1}, carrier gas = air.

340 nm. We conclude that both AM-13 and AM-14 might contain some V(V) (particularly the former). According to the Raman data, AM-13 might contain V═O bonds and does not show the peak characteristic of VO_6. On the basis of these observations and the DR UV−vis evidence, we conclude that, in AM-13, V(IV) might be in a square-pyramidal coordination.

Catalytic Tests. *2-Propanol Reaction*. A preliminary characterization of the acid−base properties of AM-13 and AM-14 was performed by means of 2-propanol conversion, a probe reaction that is tailored for both acidity and basicity.[23] The main products of this catalytic process are propene and acetone resulting from acid-catalyzed dehydration and base-catalyzed dehydrogenation, respectively. The conversions and product selectivities are given in Table 4 and indicate that AM-14 is considerably more basic and less active than AM-13.

Ethanol Oxidation. Vanadium-substituted molecular sieves are excellent catalysts in many selective oxidation reactions.[24,25] The oxidation activity of the two novel microporous vanadosilicates was studied using ethanol oxidation as a model reaction.[26] The main products formed at temperatures up to 300 °C were acetaldehyde, ethyl acetate, ethene, and diethyl ether. The ethanol oxidation activities and product selectivities are shown in Table 4. AM-13 and AM-14 exhibit similar activities, and the two catalysts have high selectivities for acetaldehyde (85.0 and 57.4%, respectively) at 300 °C. Acetaldehyde results from ethanol oxidative dehydrogenation, and these results suggest that AM-14 seems to have a higher redox activity than AM-13. For AM-13, acetaldehyde is still a major product, although the selectivity for the dehydration products ethene and diethyl ether is considerable.

After being used in the 2-propanol and ethanol reactions, AM-13 and AM-14 catalysts were characterized by powder XRD. It was found that, whereas AM-13 loses only some crystallinity, AM-14 is almost completely destroyed in both processes, so that, clearly, its potential use as a catalyst is likely to be limited.

Conclusions

In conclusion, we report the successful synthesis of two novel large-pore sodium vanadosilicates, AM-13 and AM-14, with framework composition $HNaCa_2Si_{10}VO_{47}$ and $Na_2Si_4VO_{11}$, respectively. In the as-prepared samples, both V(IV) and V(V) simultaneously occur in different coordinations, and AM-14, like AM-6, contains essentially hexacoordinated V(IV), whereas V(IV) in AM-13 might be in a square-pyramidal coordination. Preliminary catalytic characterization shows that these two vanadosilicates exhibit interesting redox properties.

Acknowledgment. The authors thank FCT, PRAXIS XXI, POCTI, and FEDER (Portugal) and EPRSC (U.K.) for financial support. We acknowledge the referees for useful comments.

CM010613Q

(23) Hathaway, P. E.; Davies, M. E. *J. Catal.* **1989**, *116*, 263.
(24) Kumar, P.; Kumar R.; Pandey, B. *Synlett* **1995**, *16*, 289.
(25) Arends, J. I. W. C. E.; Sheldon, R. A.; Wallau, M. W.; Schuchardt, V. *Angew. Chem., Int. Ed. Engl.* **1997**, *36*, 1144.
(26) Miller, J. M.; Lakshmi, L. J. *J. Catal.* **1999**, *184*, 68.